Published in final edited form as:
Toxicol Appl Pharmacol. 2009 November 15; 241(1): 61–70. doi:10.1016/j.taap.2009.08.002.

Effects of phenol on barrier function of a human intestinal epithelial cell line correlate with altered tight junction protein localization

Ingrid C. McCall[a,b,*], **Abigail Betanzos**[b], **Dominique A. Weber**[b], **Porfirio Nava**[b], **Gary W. Miller**[a], and **Charles A. Parkos**[b,*]

[a]Department of Environmental and Occupational Health, Rollins School of Public Health, Emory University, Atlanta, GA 30322, USA

[b]Department of Pathology and Laboratory Medicine, Epithelial Pathobiology Research Unit, Emory University, Atlanta, GA 30322, USA

Abstract

Phenol contamination of soil and water has raised concerns among people living near phenol-producing factories and hazardous waste sites containing the chemical. Phenol, particularly in high concentrations, is an irritating and corrosive substance, making mucosal membranes targets of toxicity in humans. However, few data on the effects of phenol after oral exposure exist.

We used an in vitro model employing human intestinal epithelial cells (SK-CO15) cultured on permeable supports to examine effects of phenol on epithelial barrier function. We hypothesized that phenol disrupts epithelial barrier by altering tight junction (TJ) protein expression. The dose-response effect of phenol on epithelial barrier function was determined using transepithelial electrical resistance (TER) and FITC-dextran permeability measurements. We studied phenol-induced changes in cell morphology and expression of several tight junction proteins by immunofluorescence and Western blot analysis. Effects on cell viability were assessed by MTT, Trypan blue, propidium iodide and TUNEL staining.

Exposure to phenol resulted in decreased TER and increased paracellular flux of FITC-dextran in a dose-dependent manner. Delocalization of claudin-1 and ZO-1 from TJs to cytosol correlated with the observed increase in permeability after phenol treatment. Additionally, the decrease in TER correlated with changes in the distribution of a membrane raft marker, suggesting phenol-mediated effects on membrane fluidity. Such observations were independent of effects of phenol on cell viability as enhanced permeability occurred at doses of phenol that did not cause cell death. Overall, these findings suggest that phenol may affect transiently the lipid bilayer of the cell membrane, thus destabilizing TJ-containing microdomains.

Keywords

Phenol; SK-CO15 cells; Transepithelial electrical resistance; Tight junctions; Epithelial paracellular barrier; Cell viability

*Corresponding authors. Department of Pathology and Laboratory Medicine, Whitehead Biomedical Research Building, Room 115, Emory University, 615 Michael Street, Atlanta, GA 30322, USA. Fax: +1 404 727 8538.

We declare no competing financial interests.

Appendix A. Supplementary data

Supplementary data associated with this article can be found, in the online version, at doi:10.1016/j.taap.2009.08.002.

Introduction

Phenol (C_6H_5OH)is a monosubstituted aromatic hydrocarbon used to manufacture phenolic resins and plastics used in fertilizers, paints, textiles, adhesives, paper, and disinfectants. Due to its anesthetic effects, phenol is also widely used in pharmaceutical products such as ointments, ear and nose drops, cold sore lotions, throat lozenges and sprays, and antiseptic lotions (Darisimall, 2006). It can be found in low concentrations in many over-the-counter products including topical preparations, mouthwashes and gargles (ATSDR, 2007a).As a result of its widespread use, phenol has been detected in at least 595 of 1,678 National Priorities List (NPL) hazardous waste sites in the United States (HazDat, 2006). In addition to its use in many household products, phenol contamination of soil and water is a concern for people living near factories producing or using phenol as well as those residing near hazardous waste sites (Chen, 1995; Clark, 1977; Plumb, 1987). Phenol, particularly in high concentrations, is an irritating and corrosive substance, making mucosal membranes targets of toxicity in humans and animals. Fatalities due to ingestion have been reported (Boatto et al., 2004; Cronin, 1949; Soares, 1982; Stajduhar-Cazic, 1968; Tanaka et al., 1998). Estimated lethal oral doses of phenol in adults vary widely, from 1 g (14 mg/kg, assuming an adult body weight of 70 kg) to as much as 65 g (930 mg/kg, assuming an adult body weight of 70 kg) (Bruce and Neal, 1987; Deichmann, 1981).

To protect the communities that reside around these areas, the U.S. Environmental Protection Agency has set a limit of 2 mg/l (21 μM) in water and also requires that spills of 1,000 pounds or more of phenol released into the environment be reported to the agency. The Clean Water Act permissible level for ambient water is 0.3 mg phenol/l (USEPA, 1980). Acute oral ingestion of large doses of phenol have been reported to cause mucosal necrosis in the mouth, esophagus and stomach along with pain, vomiting, and bloody diarrhea (Gosselin et al., 1984). Studies of populations whose drinking water was contaminated with phenol found elevated incidences of diarrhea, nausea, mouth sores, and dark urine (Baker et al., 1978; Jarvis et al., 1985).

These observations underscore the importance of understanding how phenol affects mucosal membranes as a target tissue after ingestion. Mucosal surfaces are covered by a layer of epithelial cells that regulate absorption and secretion of water, ions and nutrients while serving as a protective barrier. The regulation of epithelial barrier function is determined largely by intercellular junctions. These cell–cell junctions are composed of several multiprotein complexes assembled at distinct positions within the lateral plasma membrane in areas of cell–cell contacts comprising tight junctions (TJ), adherens junctions (AJ) and desmosomes (Matter and Balda, 2003; Tsukita et al., 2001). Tight junctions form intercellular seals that regulate the passage of fluid electrolytes, macromolecules and cells through paracellular pathways. TJs have a complex molecular composition that includes several transmembrane proteins such as claudin family members, occludin and JAM-A. Such transmembrane components are linked to cytoplasmic scaffold/signaling complexes that play important roles in regulating a number of cellular functions independent of barrier function including cell proliferation and differentiation. Indeed, signal transduction events emanating from intercellular junctions alter gene expression in the nucleus and loss of these junctional proteins has been implicated in malignant transformation and tumor metastasis (Gonzalez-Mariscal, 2005; Michael et al., 1989).

Organic compounds that share reactive groups with phenol, such as ethanol through an OH group and polychlorinated biphenyls (PCBs) with the presence of benzene rings, have been shown to alter permeability of epithelia by mediating selective alterations of TJ protein expression (Eum et al., 2008; Zhang et al., 2007). Furthermore, it has been reported that phenols have a direct toxic effect on human colonic epithelial cells in vitro (Pedersen and Saermark,

2002). Previous data for humans exposed to phenol by ingestion are inadequate to establish dose–response relationships and are needed to identify adverse effect levels. There is no sufficient data on phenol absorption into the body after oral exposure. We hypothesized that phenol may disrupt epithelial barrier by altering tight junction proteins, as these proteins maintain the architectural integrity of the epithelial layer, preserve the transcellular transport, and prevent the passage of molecules and ions through the paracellular space.

Materials and Methods

Reagents

Phenol was obtained from Fisher Scientific (Fair Lawn, NJ). Fetal bovine serum (FBS) and high-glucose Dulbecco's modified Eagle's medium (DMEM) were purchased from GIBCO BRL (Grand Island, NY). Hank's balanced salt solution buffer (HBSS) and propidium iodide (PI) were obtained from Sigma-Aldrich (St. Louis, MO). Cell Proliferation Kit I MTT (3-(4,5-dimethylthiazol-2-yl)-2,5-diphenyltetrazolium bromide) was obtained from Roche (Mannheim, Germany). Rabbit polyclonal (pAb) anti-occludin, anti-ZO-1, anti-claudin-1, anti-claudin-3 and anti-JAM-A were purchased from Zymed Laboratories (San Francisco, CA). Mouse monoclonal (mAb) anti-occludin (Zymed), anti-ZO-1, anti-JAM-A mAb was generated in house and previously described (Parkos et al., 2002), and anti-actin mAb (Sigma-Aldrich) was also used. Horseradish peroxidase (HRP) goat anti-mouse and anti-rabbit were obtained from Jackson Immunoresearch Laboratories (West Grove, PA), and donkey Alexa-488 anti-rabbit and Alexa-538 anti-mouse were purchased from Molecular Probes (Eugene, OR).

Cell culture

SK-CO15, a transformed human colonic epithelial cell line that rapidly polarizes within 5–7 days creating high-resistance (>1,000 Ohm×cm^2) monolayers, has been shown to be a good model to study tight junctions in the intestinal epithelium and was a gift from Dr. Enrique Rodriguez-Boulan (Weill Medical College of Cornell University, New York, NY; Severson et al., 2009; Mandell et al., 2005; Ivanov et al., 2006; Betanzos et al., 2009). SK-CO15 cells were grown in DMEM supplemented with 10% fetal bovine serum, 2 mM L-glutamine, 15 mM HEPES, 1% nonessential amino acids, 40 μg/ml penicillin and 100 μg/ml streptomycin, pH 7.4 as previously described (Lisanti et al., 1989).

Transepithelial electrical resistance (TER)

SK-CO15 cells were grown for 6–10 days (>1,000 Ohm×cm^2) on collagen-coated permeable polycarbonate filters with a surface area of 0.33 cm^2 and 0.4 μm pore size (Costar, Cambridge, MA). Two days after cells reached confluence, different concentrations (1 μM, 100 μM, 1 mM, 3.2 mM, 6.4 mM, 10.6 mM, 15.9 mM, 21.2 mM) of phenol were added to the apical side of the monolayers. TER of epithelial monolayers was measured at 5, 10, 15, 20, 30, 60, 120, and 180 min in the continuous presence of phenol using an EVOMX electrovoltmeter with an STX2 electrode (World Precision Instruments, Sarasota, FL). Six independent experiments on six filters each were performed.

Paracellular flux assay

SK-CO-15 cells were prepared on transwell filters as described above. When the TER was stable for 2 days, cells were rinsed three times with HBSS and incubated with HBSS for 2 h. Then, monolayers were incubated with 10.6 mM phenol for 120, 60, 30, and 10 min. After phenol treatment 10 μl of the tracer solution (10 μg/μl FITC-dextran of 4 kDa; Sigma-Aldrich, Number FD4) was added to the apical side of cells. Over a 3-h incubation with constant agitation at 37 °C, medium from the bottom chamber was collected at regular intervals and the amount of diffused dextran was measured in a fluorometer (excitation wavelength = 492 nm

and emission wavelength = 520 nm). Three independent experiments in six filters each were performed.

Cellular lysis

SK-CO15 cells were grown on six-well plates until they reached 100% confluency, then rinsed three times with HBSS, and incubated with HBSS for 2 h at 37 °C. Subsequently, 3.2, 10.6, 21.2 mM of phenol were added for 10 and 60 min. Cells were rinsed three times with HBSS supplemented with 1 mM PMSF (phenylmethylsulfonyl fluoride) and homogenized in RIPA (radioimmunoprecipitation assay) lysis buffer (20 mM Tris, 50 mM NaCl, 2 mM EDTA, 2 mM EGTA, 1% sodium deoxycholate, 1% TritonX-100, and 0.1% SDS, pH 7.4) containing 1 mM PMSF and proteinase inhibitors cocktail (Sigma-Aldrich). Cells were scraped and transferred to an Eppendorf tube followed by incubation with agitation for 10 min at 4 °C. The samples were sonicated twice for 10 s, and nuclei and cell debris were cleared by centrifugation at 4 °C for 10 min at 13,000 rpm. Total protein content in the supernatant was quantified using a BCA kit (Thermo Scientific, Rockford, IL). Samples were diluted with reducing sample buffer (250 mM Tris–HCL, 30% glycerol, 10% SDS, 20% B-mercaptoethanol, 0.012% bromophenol blue) and boiled for 5 min prior to SDS-PAGE.

Immunoblotting

Equal amounts of cellular lysates were separated by SDS-PAGE in8%, 10%, 12% and 15% gels depending on the size of the protein of interest, followed by overnight (ON) transfer to polyvinylidene difluoride (PVDF) membranes (Bio-Rad, Hercules, CA). Nonspecific binding was blocked using 5% nonfat milk in Tween Tris-buffered saline (TTBS) for 1 h at room temperature (RT). Membranes were incubated ON with the following primary antibodies (stock solutions were 0.25 mg/ml) diluted in blocking solution: pAb anti-occludin (1:500), pAb anti-claudin-1 (1:100), pAb anti-ZO-1 (1:250), pAb anti-JAM-A (1:1,000), pAb anti-claudin-3 (1:1,000) and anti-actin (1:2,000). After three washes with TTBS for 5 min each, membranes were incubated with species-specific HRP-conjugated secondary antibodies for 1 h at RT, followed by three washes with TTBS and one wash with TBS for 5 min. Blots were developed using a BM chemiluminescence blotting substrate (POD) kit (Roche, Indianapolis, IN), HyBlot autoradiography films (Denville, Metuchen, NJ) and a developer instrument (Konica Minolta, New Jersey, NJ) were used. Densitometry analyses were performed by using ImageJ program.

Immunofluorescence labeling

SK-CO15 cells were plated on coverslips and when they reached 100% confluency were treated with phenol at 3.2, 10.6, and 21.2 mM for 10and 60 min. After washing with HBSS, cells were fixed and permeabilizedin absolute ethanol for 20 min at −20 °C, followed by blocking in 3% BSA for 60 min at RT. Coverslips were incubated overnight with primary mAb as follows: anti-occludin (1:100), anti-ZO-1 (1:100), anti-claudin-1 (1:25), anti-JAM-A (1:200) and anti-claudin-3 (1:250). After rinsing three times with HBSS, the preparations were incubated with Alexa-488 or Alexa-538 labeled secondary antibody for 1 h at RT under dark conditions. Three washes with HBSS were performed and slides were mounted with Prolong Antifade medium (Molecular Probes). Stained cell monolayers were examined using a Zeiss LSM510 laser scanning confocal microscope (Zeiss Microimaging, Inc., Thomwood, NY) coupled to a Zeiss 100 M axiovert and 63× or 100× Pan-Apochromat oil lenses.

Terminal deoxynucleotidyl transferase UTP nick end labeling (TUNEL)

We detected apoptosis using the TUNEL technique (*In situ* Cell Death Detection Kit, Roche, Indianapolis, IN). SK-CO15 cells were plated on 0.4-μm filters (0.33 cm^2) and at confluency phenol was added to the culture at final concentrations of 3.2, 10.6, and 21.2 mM for 10 and 60 min. Subsequently, cells were washed twice with HBSS, fixed and permeabilized in absolute

ethanol for 20 min at −20 °C. Filters were incubated with 50 µl TUNEL reaction mixture for 60 min at 37°C in the dark. Then, three washes with HBSS were done and slides were mounted with prolong antifade medium. Stained cell monolayers were examined using an excitation wavelength in the range of 450– 500 nm and detection in the range of 515–565 nm (green).

Propidium iodide (PI) labeling

We performed the supravital propidium iodide (PI) assay that can identify cells that have altered membrane permeability. PI intercalates into double-stranded nucleic acids when it penetrates the cell membranes of dying or dead cells (Zamai et al., 2001). SK-CO15 cells were plated in 25 cm^2 culture flasks and, after 2 days of confluency, were washed twice with HBSS and incubated in HBSS for 2 h. Subsequently, phenol was added to the culture at final concentrations of 3.2, 10.6, 21.2 for 10 and 60 min. The adherent cells were rinsed twice with PBS and harvested by standard trypsinization (0.5 mg/ml trypsin and 0.2 mg/ml EDTA in PBS; Sigma-Aldrich). Detached cells were collected with the supernatants, pelleted by centrifugation, and washed with FACS buffer (PBS supplemented with 2% FBS and containing 0.1% NaN_3). The pelleted cells were resuspended in 1 ml FACS buffer with 2 µg/ml PI and then analyzed by flow cytometry. The flow analysis was performed by a FACScan (Becton Dickinson) equipped with an argon ion laser tuned at 488 nm wavelength. Data analysis was performed with CellQuest software (Becton Dickinson).

MTT assay

We performed the MTT assay to assess cell viability by staining metabolically active cells. SK-CO15 cells were grown on 96-well plates until reaching100% confluence followed by rinsing three times with HBSS and incubation in the same buffer for 2 h at 37 °C. Subsequently, various concentrations of phenol were added, and 10 and 60 min later10 µl of the MTT labeling reagent was added and incubated for 1 h at 37 °C. Solubilization solution was added (100 µl/well), and data were analyzed by spectrophotometry in a microtiter plate reader at a wavelength of 590 after overnight incubation at 37 °C.

Lipid layer integrity using FITC-labeled cholera toxin B

SK-CO15 cells were plated on coverslips and when they reached 100% confluence were treated with phenol at 21.2 mM for 10 min. After washing with HBSS, cells were labeled in suspension with 2 µg/ml of FITC-labeled cholera toxin B apically to distinguish the lipid layer rich in sphingolipids and cholesterol. Cells were fixed/permeabilized with ethanol and stained for the tight junction occludin. Stained cell monolayers were examined using a Zeiss LSM510 laser scanning confocal microscope (Zeiss Microimaging, Inc., Thomwood, NY) coupled to a Zeiss 100 M axiovert and 63 or 100 Pan-Apochromat oil lenses.

Results

Phenol exposure results in a rapid decrease in TER in a dose-dependent manner that is transient

Disruption of epithelial barrier function can be measured by changes in TER. Confluent monolayers (500–1,000 Ohm×cm^2) of the transformed human colonic epithelial cell line SK-CO15 were treated with increasing concentrations of phenol, ranging from 1 µM to 21.2 mM. Measurements of TER were performed over a 3-h time course. As shown in Fig. 1, the TER decreased in a dose-dependent manner with increasing concentrations of phenol. As can be seen, the phenol effect was very brisk as a significant decrease in TER was observed within 5 min at concentrations above 1 mM. The maximum effect of phenol was observed at 10 min of exposure. However, the paracellular barrier alteration caused by phenol was transient since TER began to recover within 30 min of treatment. Therefore, treatment of cells with phenol

suggests that there is reversible disruption of epithelial barrier at early times after exposure even at very low phenol concentrations.

Phenol increases the paracellular flux

FITC-dextran (4 kDa) is small enough to diffuse through the paracellular space when junctions are perturbed. We thus used FITC-dextran flux as a measure to confirm whether phenol specifically affected paracellular barrier function in epithelial cells. As shown in Fig. 2, SK-CO15 cells exposed to 10.6 mM phenol for 120, 60, 30, and 10 min showed a significant increase in flux of FITC-dextran compared to controls. These results suggest that phenol significantly increases epithelial paracellular permeability in vitro.

Internalization of claudin-1 and delocalization of ZO-1 from TJ are associated with phenol-induced increases in epithelial permeability. Since TJ proteins regulate paracellular flux, we examined the localization of TJ-associated proteins occludin, claudin-1, claudin-3, JAM-A, and ZO-1 in epithelial SK-CO15 cells after treatment with phenol by immunofluorescence (Fig. 3–Fig. 4). As shown in Fig. 3A, exposure to 3.2 mM phenol for 10 min did not significantly alter the immnunostaining for claudin-1 protein. However, after exposure for 10 and 60 min to 10.6 and 21.2 mM of phenol, there was an increase in claudin-1 cytoplasmic staining (punctuate dots) in comparison to control cells. These data suggest that claudin-1 may be internalized from the membrane after the phenol exposure. Similar results were observed for ZO-1 as is indicated in Fig. 3B. After phenol treatment, ZO-1 showed a marked decrease in the junctional labeling. In contrast, at all concentrations of phenol tested, there were no significant alterations in the junctional staining patterns of occludin (Fig. 4A), claudin-3 (Fig. 4B) and JAM-A (Fig. 4C). These results suggest that changes in paracellular permeability observed by phenol treatment correlate with delocalization of claudin-1 and ZO-1 from TJ to cytosolic pools.

Total cellular levels of TJ proteins are not modified by phenol

Since we observed changes in TJ protein localization, the effects of phenol on protein expression levels were examined. Thus, we analyzed the amount of TJ proteins by Western blot after phenol treatment. As shown in Fig. 5, total cellular lysates of SK-CO15 cells treated with different concentrations of phenol were employed to immunodetect the expression of occludin, claudin-1, claudin-3, and ZO-1, as well as, actin as a loading control. Interestingly, phenol treatment did not significantly affect the total level of expression of any TJ-associated proteins as determined by staining densitometry (data not shown). These findings suggest that changes in localization of some TJ proteins by phenol treatment were not reflected by altered levels of protein expression.

Cellular viability is not reduced by phenol exposure

In order to determine the mechanism of altered barrier function after phenol treatment, SK-CO15 cells were screened for effects on levels of apoptosis and necrosis. To assess apoptosis, cells were harvested when phenol-induced changes in TER were observed and probed for the apoptosis marker poly-(ADP-ribose)-polymerase (PARP) by Western blot (Fig. 6A). PARP is a major target for cleavage by active caspase-3, which in turn is cleaved by caspase-9. We observed that the protein band corresponding to the large PARP fragment was enhanced after phenol treatment when compared to control (no phenol added). To corroborate these findings, we performed TUNEL staining to detect apoptotic cells (Fig. 6B). SK-CO15 cells treated with phenol displayed more than a two-fold increase in TUNEL labeling, compared with the control, especially at early times of phenol exposure (10 min). We tested whether an apoptosis inhibitor might protect cells from phenol-induced effects on cell viability, the caspase inhibitor Z-VAD was added to the cells before phenol treatment (Fig. 6C). As can be shown, the inhibitor Z-VAD protected phenol-treated SK-CO15 cells from apoptosis as assessed by TUNEL labeling.

In order to also evaluate if the disruption of epithelial barrier caused by phenol is mediated by enhanced apoptosis, the inhibitor Z-VAD was employed and TER was evaluated. The results in Fig.7 show that Z-VAD did not reverse the decreased in TER caused by phenol, suggesting that impaired barrier function is independent of apoptosis.

To assess whether phenol induces cellular necrosis, propidium iodide (PI) staining followed by flow cytometry was performed on SK-CO15 cells treated with phenol. As shown in Fig. 8, SK-CO15 cells treated with 3.2, 10.6 and 21.2 mM of phenol displayed 16%, 30%, and 59% increases in PI labeling, respectively, after 60 min of phenol treatment.

However, as shown in Fig. 9, SK-CO15 cells treated with different concentrations of phenol displayed no significant increase of MTT labeling after 10 and 60 min of treatment suggesting that phenol does not compromise cell viability.

The above results suggested that the effects of phenol on barrier function are independent of effects on cell viability. Furthermore, the enhanced staining with propidium iodide after phenol treatment could be explained by direct effects on membrane permeability/ fluidity. Since TJ function and hence permeability has been linked to partitioning of junction components into lipid raft containing membrane microdomains, we assessed whether phenol treatment alters distribution of a marker of lipid rafts. For this experiment, SK-CO15 cells were stained with FITC, labeled cholera toxin before and after phenol treatment. As can be seen in Fig. 10, there is a marked reduction in apical membrane staining for cholera toxin after phenol treatment suggesting alteration of the cholesterol-rich microdomains that contain the receptor for cholera toxin.

Discussion

Epithelial layers are formed by closely apposed polarized cells that form contacts with adjacent cells through specialized intercellular junctions comprised, in part, by tight junctions. The primary function of TJs is to act as a barrier between the lumen of the intestine and the internal milieu. This highly selective barrier allows for paracellular flux and represents a key defense from ingested toxicants. Phenol is a pervasive toxicant with known human health effects after ingestion. Previous work has shown that phenols can significantly impair the viability of primary human colonic epithelial cell cultures HT-29 cells (Pedersen and Saermark, 2002). However, little is known about the mode of interaction between phenol and epithelial cells.

To further examine how phenol affects the mucosa after oral exposure, we studied the effect of phenol on epithelial monolayers. We first performed dose response and time course experiments of epithelial paracellular barrier function after phenol exposure. Our data showed that treatment of epithelial cells with phenol results in enhanced paracellular permeability in a dose-dependent manner. We observed that concentrations lower than 100 μM have little effect on epithelial barrier function. Furthermore, concentrations between 1 and 10 mM of phenol after 5 min significantly decreased the TER in intestinal epithelial monolayers; however, this alteration was reversible to control values after 2 h. Moreover, at high concentrations, we observed that recovery of monolayers was not complete even after 3 h of exposure (Fig. 1). The phenol-induced decreases in TER correlated with significant increases in apical-to-basal flux of an extracellular fluorescent-marker FITC-dextran (Fig. 2). Our data showed that dramatic differences of paracellular barrier integrity, measured by TER, were dose dependent and increased with length of exposure. We also observed that recovery after exposure was time dependent. Accordingly, we determined the optimal concentrations and times of exposure used in later experiments.

Since TJ proteins are involved in the maintenance of epithelial barrier function, our observations that phenol increases paracellular permeability *in vitro* led us to investigate the

role of TJ-associated proteins claudin-1, claudin-3, occludin, JAM-A, and ZO-1. These proteins are known to be directly involved in regulation of paracellular barrier function (Tsukita et al., 2001; Furuse et al., 2002). Three integral membrane proteins have been shown to play a role in regulating TJ function; occludin, claudins and JAMs. The former two constitute the backbone of TJ strands (González-Mariscal, 2003). In experimental conditions, impairment of the paracellular barrier function has often been related to alterations in the junctional expression and localization of occludin and claudins (Collares-Butazo et al., 1998a, 1998b; Tsukita et al., 2002). Both occludin and claudins bind to a complex of cytoplasmic proteins (e.g., ZO-1, ZO-2, ZO-3, cingulin, 7H6 antigen, symplekin and others) that have been identified in the cytoplasmic submembraneous plaque underlying membrane contacts. These proteins appear to organize the occludin and claudin complexes within the TJ region and couple them to actin microfilaments (Fanning et al., 1998; Itoh et al., 1999; Schneeberger et al., 2004). It is expected that changes on ZO-1 localization would affect its transmembrane binding partners such as occludin and claudins; however, our data suggest that phenol affects the localization only of ZO-1 and claudin-1 but not occludin (Fig. 4A). It is known that ZO-1 binds both to occludin and claudin, yet the nature of these interactions has not been determined. Perhaps the differences we observed in the effects of phenol are secondary to differences in the binding strength and/or the stoichiometry of these interactions with ZO-1-claudin-1. Additionally, since occludin binds strongly to actin through its C-terminus, it is possible that phenol does not affect this interaction and thus does not affect occludin. However, further studies are necessary to determine the molecular basis of these findings.

Our results suggest that changes in paracellular permeability observed by phenol treatment were caused by delocalization of claudin-1 and ZO-1 from TJ and translocation to the cytosol (Fig. 3). One possible mechanism is that phenol-induced effects are secondary to changes in the cell membrane (Fig. 10), which result in disruption of TJ-containing microdomains. Disruption of these microdomains would result in transient mislocalization of TJ components and altered paracellular pathway (Nusrat et al., 2000).

The damage observed by phenol exposure could also be due to effects on cell viability. This hypothesis was tested by evaluating the level of apoptosis and necrosis in phenol-treated epithelial cells. We examined whether the cells underwent apoptosis or necrosis at times when differences in TER were observed. Not surprisingly, we observed increase in apoptosis by TUNEL staining (Fig. 6B) and necrosis by PI (Fig. 8) and by Trypan blue (Supplemental Fig. 1) on epithelial cells exposed to phenol when compared to control. Interestingly, we observed that cell viability was not compromised as assessed by MTT (Fig. 9) when compared to control, suggesting that such increases in labeling with cell impermeant dyes such as PI and Trypan blue were not accompanied by altered cell viability as determined by MTT assays, since this reagent stains metabolically active cells. The above results suggest that the observed fall in TER might be secondary to phenol-mediated effects on the cell membrane. We speculate that at low doses of phenol, membrane repair can occur, which would explain the recovery of the TER. High doses of phenol, on the other hand, may damage membranes sufficiently to lead to cell death.

Moreover, we observed that alterations in barrier function after phenol treatment were independent of apoptosis, or necrosis, as TER declined in cells treated with phenol in the presence of the apoptosis inhibitor Z-VAD (Fig. 7). Taken together, the above findings suggest that the decreased TER is most likely secondary to phenol-induced alterations in the cell membrane.

We showed in this study dramatic effects of phenol on the integrity of intestinal epithelial layers. It is thus important to understand how phenol exposure affects the tissues that first come in contact with this contaminant. Phenol is an important environmental and occupational hazard

because of its widespread use in industry and subsequent release into the environment. So far phenol contamination has been detected at 595 hazardous waste sites in the United States (HazDat, 2006). There are 10 facilities that produce phenol in the United States with a production capacity of approximately 6.9×10^9 pounds per year (ATSDR, 2007a). According to the Toxics Release Inventory, 85,700 pounds of phenol were released from 679 domestic processing facilities into surface water in 2004 (TRI04, 2006). Individuals are exposed to phenol through a variety of routes including inhalation, dermal absorption and ingestion of contaminated drinking water. The presence of phenol in groundwater is probably the result of release into soil from industrial sites or waste dumps (ATSDR, 2007a).

While concentrations used in this study were higher than the EPA standard (0.02 mM), they are within the range of low, medium and high concentrations of phenol detected in epidemiologic studies (Baker et al., 1978; Jarvis et al., 1985). For instance, phenol has been detected in ground and drinking water at concentrations as high as 12 mM. Furthermore,it has been reported that repeated oral exposure of relatively large doses for several weeks (estimated intake, 10– 240 mg/day) due to contamination of groundwater after an accidental spill of phenol resulted in mouth sores, diarrhea and dark urine. Cases of suicide have also been reported with ingestions of phenol as low as 1 g. (Gosselin et al., 1984; ATSDR, 2007; Michael et al., 1989).

These observations emphasize the importance of understanding how phenol affects the mucosal membranes as a target tissue.By using the *in vitro* model in this study, we suggest that exposure to phenol affects epithelial barrier function by disrupting cellular membrane domains, thus indirectly altering the distribution of TJ-associated proteins. Our results raise the concern that general populations, especially those living in areas with high phenol contamination from industrial releases or landfills, may be vulnerable to gastrointestinal dysfunction or injury due to the ability of phenol to disrupt epithelial barrier function in the gut.

Conclusion

Phenol induces diverse effects on the epithelial barrier function *in vitro*. Phenol-induced changes in TER and paracellular flux of extracellular markers were dependent on the length of exposure to phenol and the concentration employed. Based on these observations we propose that the phenol-induced effects are secondary to changes in the cell membrane resulting in disruption of TJ-containing microdomains. Disruption of these microdomains would result in mislocalization of TJ components and altered paracellular permeability. Although, low doses phenol do not compromise cell viability, at high doses, it can lead to cell death. Thus, the *in vitro* system using SK-CO15 human colonic epithelial cells provides a reasonable model for investigating the action of phenols on epithelial monolayers. Taken together, these findings suggest that cellular membrane microdomains are affected by phenol exposure, thus destabilizing the TJ proteins that regulate epithelial barrier function.

Supplementary Material

Refer to Web version on PubMed Central for supplementary material.

Abbreviations

TER	transepithelial electrical resistance
TJ	tight junctions
JAM-A	junction adhesion molecule A
ZO-1	zonula occludens 1

ZVAD	Z-Val-Ala-Asp-fluoromethylketone
TUNEL	terminal deoxynucleotidyl transferase UTP nick end labeling
PI	propidium iodide
MTT	3-(4,5-dimethylthiazol-2-yl)-2,5-diphenyltetra-zolium bromide
PARP	poly-(ADP-ribose)-polymerase
Ab	antibody

Acknowledgments

We thank Dr. Susan Voss for expert cell culture, Dr. Michael Schnoor, and Dr. Neal Beeman, and Dr. Christopher Capaldo for scientific advice. This research was performed in partial fulfillment of a MPH degree at Rollins School of Public Health at Emory University. This work was supported by the National Institutes of Health DK72564 and DK61379 (C.A.P), a Digestive Diseases Minicenter grant DK064399 (epithelial cell culture core and microscopy core support), and the Crohn's and Colitis Foundation of America (P. Nava).

References

ATSDR. Medical Management Guidelines for Phenol. Final rule. Fed. Reg 2007;66:6076–7066.

Baker ELLP, Bertozzi PE, et al. Phenol poisoning due to contaminated drinking water. Arch. Environ. Health 1978;33:89–94. [PubMed: 646461]

Betanzos A, Parkos CA, et al. Evidence for cross-reactivity of JAM-C antibodies: implications for celular localization studies. Biol. Cell 2009;101:441–453. [PubMed: 19143587]

Boatto GNM, Carta A, et al. Determination of phenol and o-cresol by GC/MS in a fatal poisoning case. Forensic Sci. Int 2004;139(2–3):191–194. [PubMed: 15040915]

Bruce RMSJ, Neal MW. Summary review of the health effects associated with phenol. Toxicol. Ind. Health 1987;3:535–568. [PubMed: 3324392]

Chen CSZJ. organic priority pollutants in wetland-treated leachates at a landfill in central Florida. Chemosphere 1995;31:3455–3464.

Clark TPPR. Chemical quality and indicator parameters for monitoring landfill leachate in Illinois. Environ. Geol 1977;1:329–340.

Collares-Butazo CBJM, McEwan GT, Hirst BH, Simmons NL. Co-culture of two MDCK strains with distinct junctional protein expression: a model for intercellular junction rearrangement and cell sorting. Cell Tissue Res 1998a;291:267–276.

Collares-Butazo CBJM, Simmons NL, Hirst BH. Increased tyrosine phosphorylation causes redistribution of adherens junction and tight junction proteins and perturbs paracellular barrier function in MDCK epithelia. Eur. J. Cell Biol 1998b;76:85–92.

Cronin TDBR. Death due to phenol contained in foille. JAMA 1949;139:777–778.

Darisimall. Sore throat lozenges and sprays. 2006 Jul 27. http://store.darisimall.com/sothlosp.html

Deichmann, WBKM. Phenols and phenolic compounds. In: Clayton, GD.; Clayton, FE., editors. Patty's industrial hygiene and toxicology. 1981. 25672627

Eum SAI, Couraud P, Hennig B, Toborek. PCBS and tight junction expression. Environ. Toxicol. Pharmacol 2008;25:234–240. [PubMed: 18438464]

Fanning ASJBJ, Jesaitis LA, Anderson JM. The tight junction protein ZO-1 establishes a link between the trasmembrane protein occludin and the actin cytoskeleton. J. Biol. Chem 1998;273:29745–29753. [PubMed: 9792688]

Furuse MTS, Hata M, Furuse K, Yoshida Y, Haratake A. Claudin-based tight junctions are crucial for the mammalian epidermal barrier: a lesson from claudin-1-deficient mice. J. Cell Biol 2002;156:1099–1111. [PubMed: 11889141]

González-Mariscal. Tight junction proteins. Prog. Biophys. Mol. Biol 2003:81.

Gosselin, RE.; Smith, RP.; Hodge, HC. Clinical Toxicology of Commercial Products. 5th ed. Baltimore: Williams and Wilkins; 1984.

HazDat. ATSDR's Hazardous Substance Release and Health Effects Database. Vol. 18. Atlanta, GA: Environ. Sci. Technol; 2006. HazDat Database: Toxicological Profile for Phenol; p. 483-490.

Itoh MFM, Morita K, Kubota K, Saitou M, Tsukita S. Direct binding of three tight junction-associated MAGUKs, ZO-1, ZO-2, and ZO-3, with the COOH termini of claudins. J. Cell Biol 1999;147:1351–1363. [PubMed: 10601346]

Ivanov A, McCall IC, et al. Microtubules regulate disassembly of epithelial apical junctions. BMC Cell Biology 2006;1:7–12.

Jarvis SNSR, Williams ALJ. Illness associated with contamination of drinking water supplies with phenol. Br. Med. J 1985;290:1800–1802. [PubMed: 3924263]

Lisanti MCI, Davitz M, Rodriguez-Boulan E. A glycophospholipid membrane anchor acts as an apical targeting signal in polarized epithelial cells. J. Cell Biol 1989;109:2145–2156. [PubMed: 2478564]

Mandell K, Babbin BA, Nusrat A, Parkos C. Junctional adhesion molecule 1 regulates epithelial cell morphology through effects on _1 integrins and Rap1 activity. J. Biol. Chem 2005;280:11665–11674. [PubMed: 15677455]

Matter K, Balda MS. Signalling to and from tight junctions. Nat. Rev. Mol. Cell Biol 2003;4:225–236. [PubMed: 12612641]

Michael P, et al. A glycophospholipid membrane anchor acts as an apical targeting signal in polarized epithelial cells. J. Cell Biol 1989;109:2145–2156. [PubMed: 2478564]

Nusrat A, et al. Tight junctions are membrane microdomains. J. Cell Sci 2000;113:1771–1781. [PubMed: 10769208]

Parkos CNA, Schnell F, Reaves T, Walsh S, Pochet M. Human junction adhesion molecule regulates tight junction resealing in epithelia. J. Cell Sci 2002;113(Pt. 13):2363–2374. [PubMed: 10852816]

Pedersen GBJ, Saermark T. Phenol Toxicity and Conjugation in Human Colonic Epithelial Cells. Scand. J. Gastroenterol 2002;37:74–79. [PubMed: 11843040]

Plumb. A comparison of ground water monitoring data from CERCLA and RCRA sites. Ground Water Monit. Rev 1987;7:94–100.

Schneeberger EELR. The tight junction: a multifunctional complex. Am. J. Physiol. Cell Physiol 2004;286:C1213–C1228. [PubMed: 15151915]

Severson EA, Parkos CA, et al. Junctional adhesión molecule A interacts with Afadin and PDZ-GEF2 to actívate Rap 1A, regulate beta1 integrin levels, and enhance cell migration. Mol. Biol. Cell 2009;7:1916–1925. [PubMed: 19176753]

Soares ERTJ. Phenol poisoning: three fatal cases. J. Forensic. Sci 1982;27:729–731. [PubMed: 7119722]

Stajduhar-Caric Z. Acute phenol poisoning. Singular findings in lethal case. J. Forensic Med 1968;15:41–42. [PubMed: 5662696]

Tanaka SCN, Kita T. Distribution of phenol in a fatal poisoning case determined by gas chromatography/mass spectrometry. J. Forensic Sci 1998;43:1086–1088. [PubMed: 9729832]

TRI04. Office of Environmental Information. Washington, DC: 2006. Providing Access to EPA's Toxics Release Inventory Data.

Tsukita S, Furuse M, Itoh M. Multifunctional strands in tight junctions. Nat. Rev. Mol. Cell Biol 2001;2:285–293. [PubMed: 11283726]

Zamai L, et al. Supravital exposure to propidium iodine identifies apoptosis on adherent cells. Cytometry 2001;44:57–64. [PubMed: 11309809]

Zhang YLQ, Guo W, Huang Y, Yang J. Effects of chronic ethanol ingestion on tight junction proteins and barrier function of alveolar epithelium in the rat. SHOCK 2007;28:245–252. [PubMed: 17515855]

USEPA. Ambient Water Quality Criteria Document: Phenol p.C-38. 1980 (U. S. E. P. Agency440-80-066, Ed.).

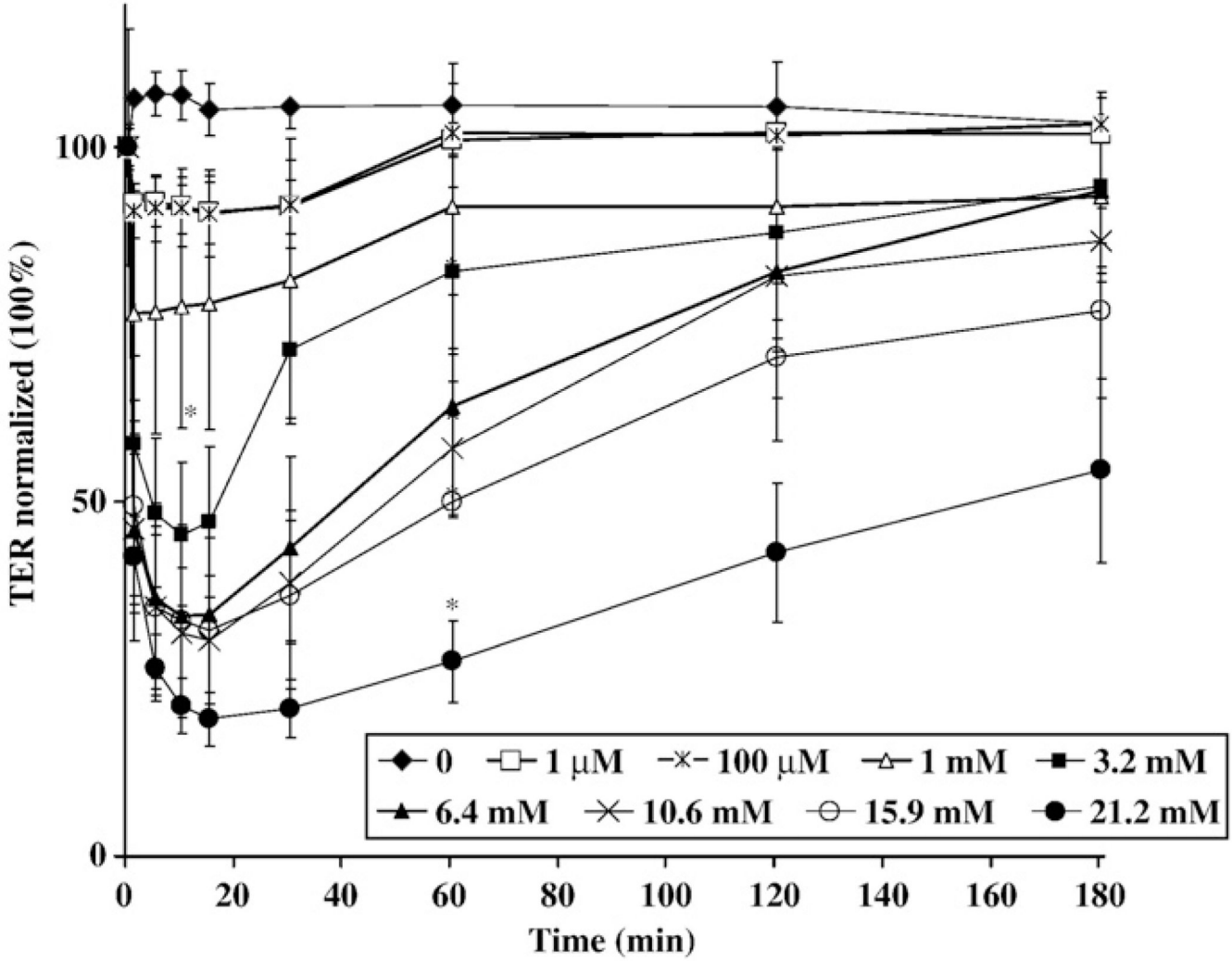

Fig. 1.

Effect of phenol on TER. TER of SK-CO15 epithelial cells was measured at 5, 10, 15, 20, 30, 60, 120, and 180 min in the continuous presence of 1 μM, 100 μM, 1mM, 3.2 mM, 6.4 mM, 10.6 mM, 15.9 mM, 21.2 mM phenol. Each point represents the average of six measurements *p<0.05 (post-test following two-way ANOVA) compared with the untreated control.

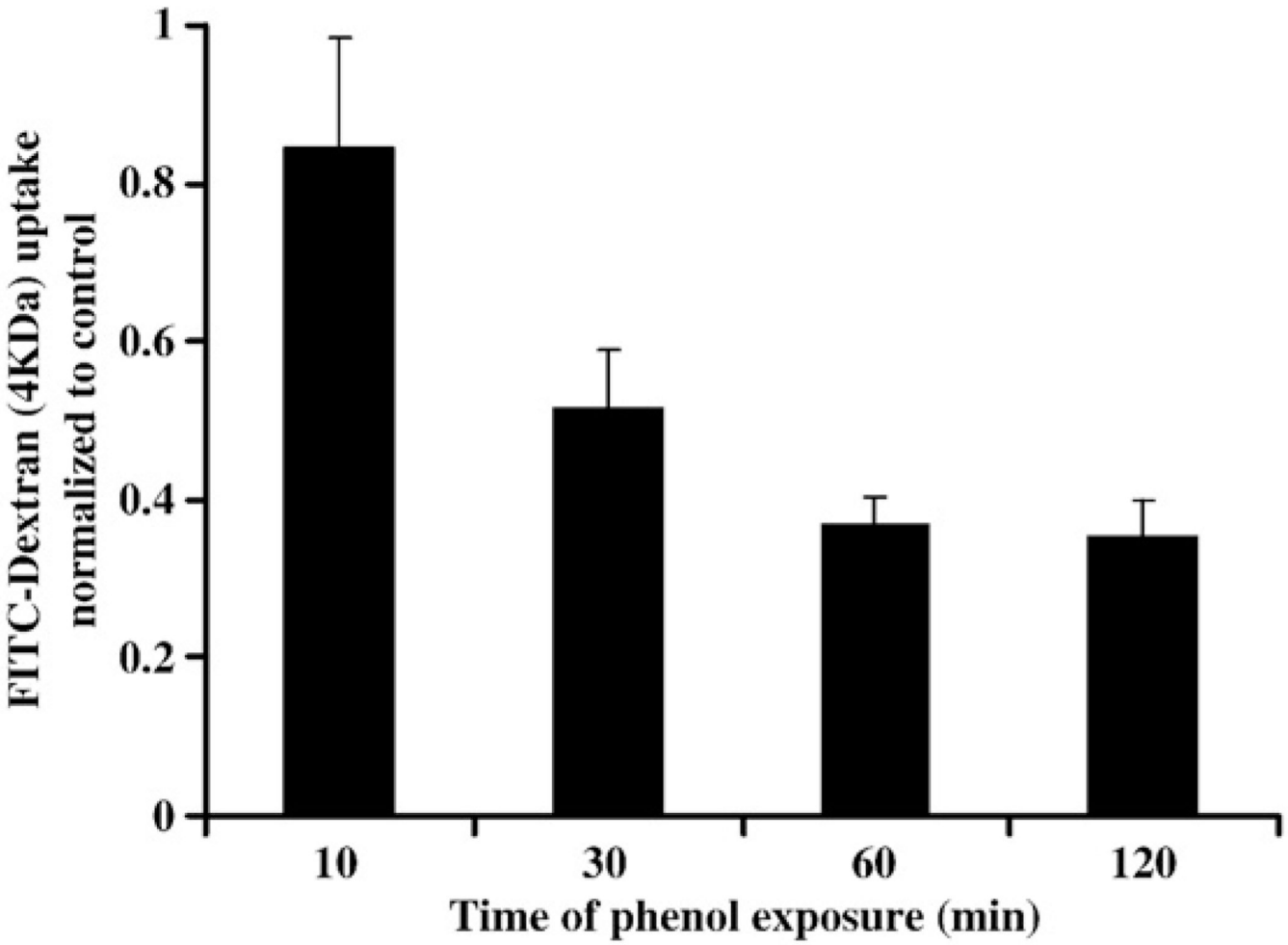

Fig. 2.

Effect of phenol on dextran flux. Paracellular flux of FITC-dextran across confluent monolayers of SK-CO15 cells was determined after 10, 30, 60 and 120 min of treatment with 10.6 mM phenol. The relative fluorescence levels indicate the average and standard error of levels of dextran in the lower chamber (diffused) for 3 h after exposure with phenol for the times indicated.

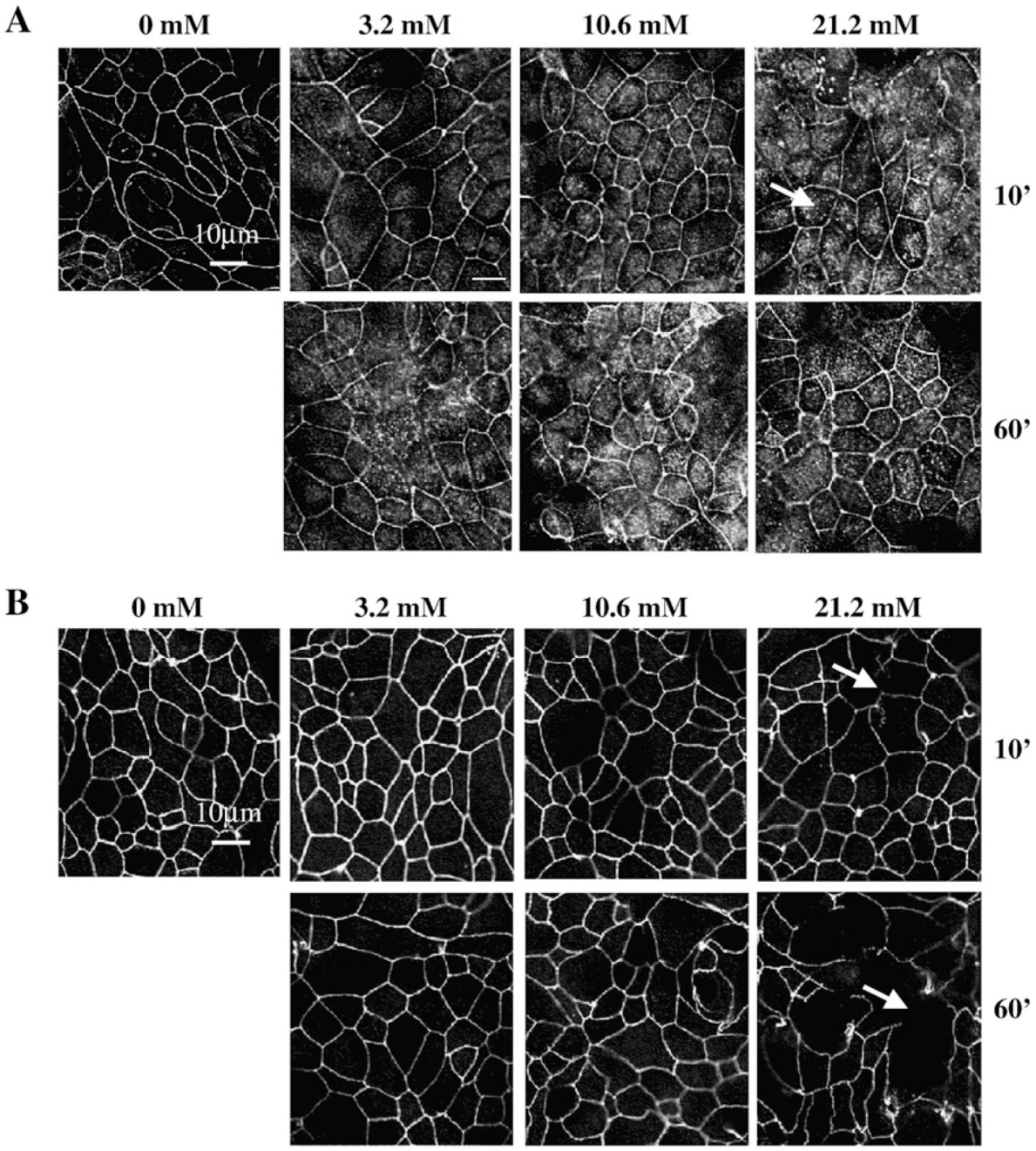

Fig. 3.

Localization of claudin-1 and ZO-1 after phenol treatment. SK-CO15 monolayers were treated with phenol (3.2, 10.6, 21.2 mM) for 10 and 60 min and immunostained by standard indirect immunofluorescence method for (A) claudin-1. Arrows indicate the cytosolic punctate labeling. (B) ZO-1. Arrowheads point to cellular membrane showing delocalization of ZO-1. Bar=10 µm.

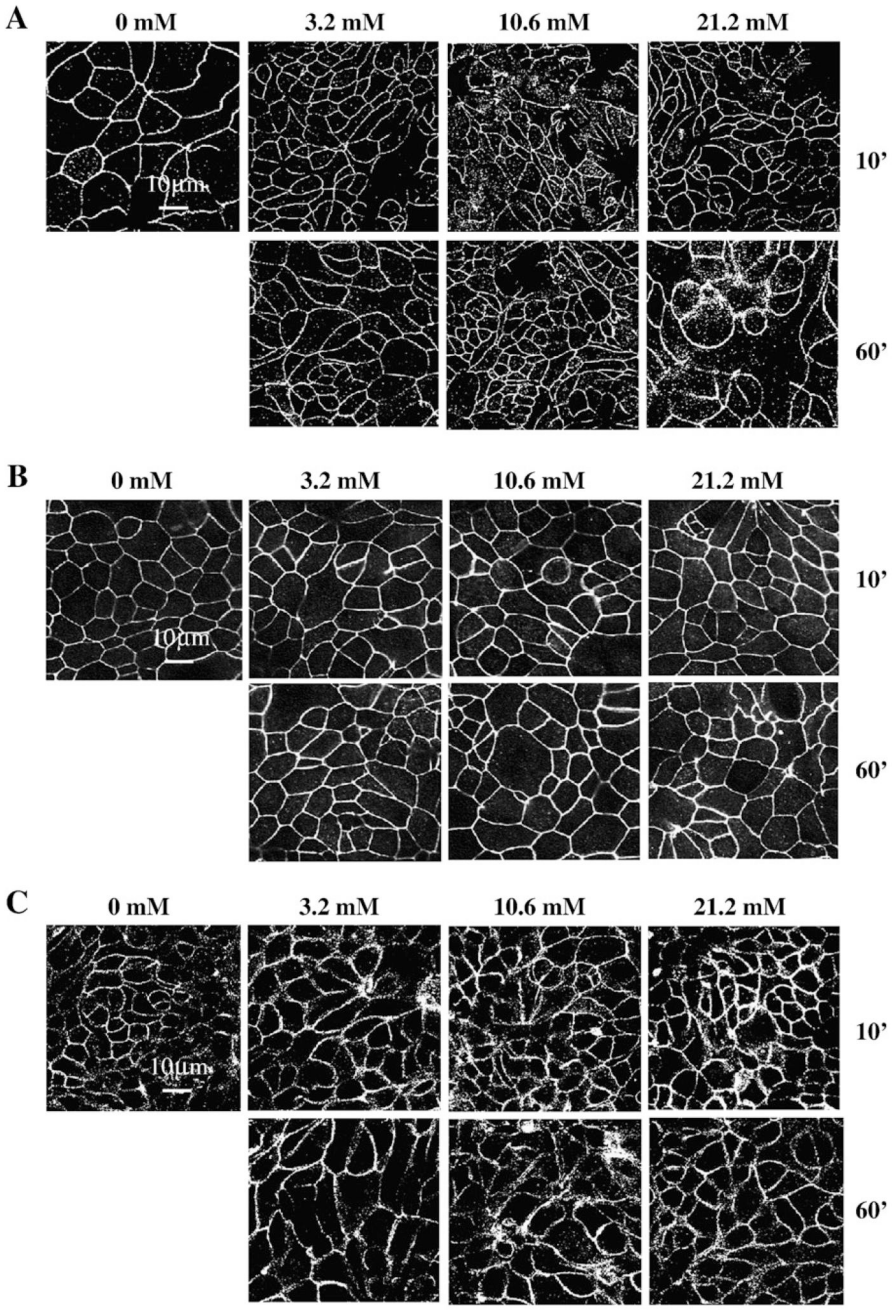

Fig. 4.

Localization of occludin, claudin-3, and JAM-A after phenol treatment. SK-CO15 monolayers were treated with phenol (3.2, 10.6, 21.2 mM) for 10 and 60 min and immunostained for (A) occludin, (B) claudin-3, and (C) JAM-A by standard indirect immunofluorescence method. Treatment with phenol had no significant effect on the junctional expression of these proteins, as compared to the controls. Bar = 10 μm.

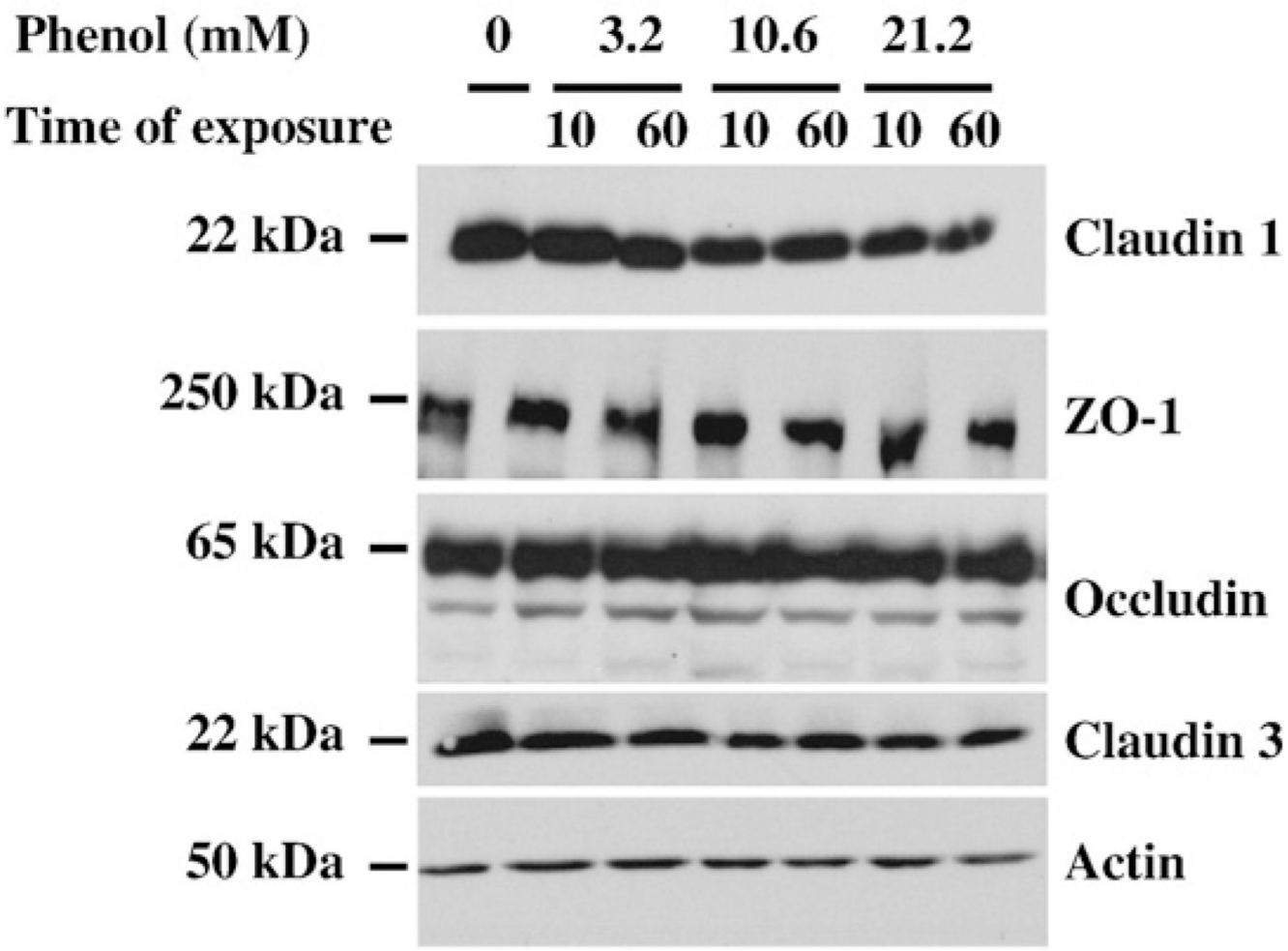

Fig. 5.

Level expression of TJ proteins after phenol treatment. Total cellular lysates from SK-CO15 treated with phenol at 3.2, 10.6, 21.2 mM for 10 and 60 min were probed for protein expression by Western blot assays and anti-claudin-1, -ZO-1, -occludin, and -claudin-3 antibodies were used. Membranes were stripped and reprobed for actin as a loading control.

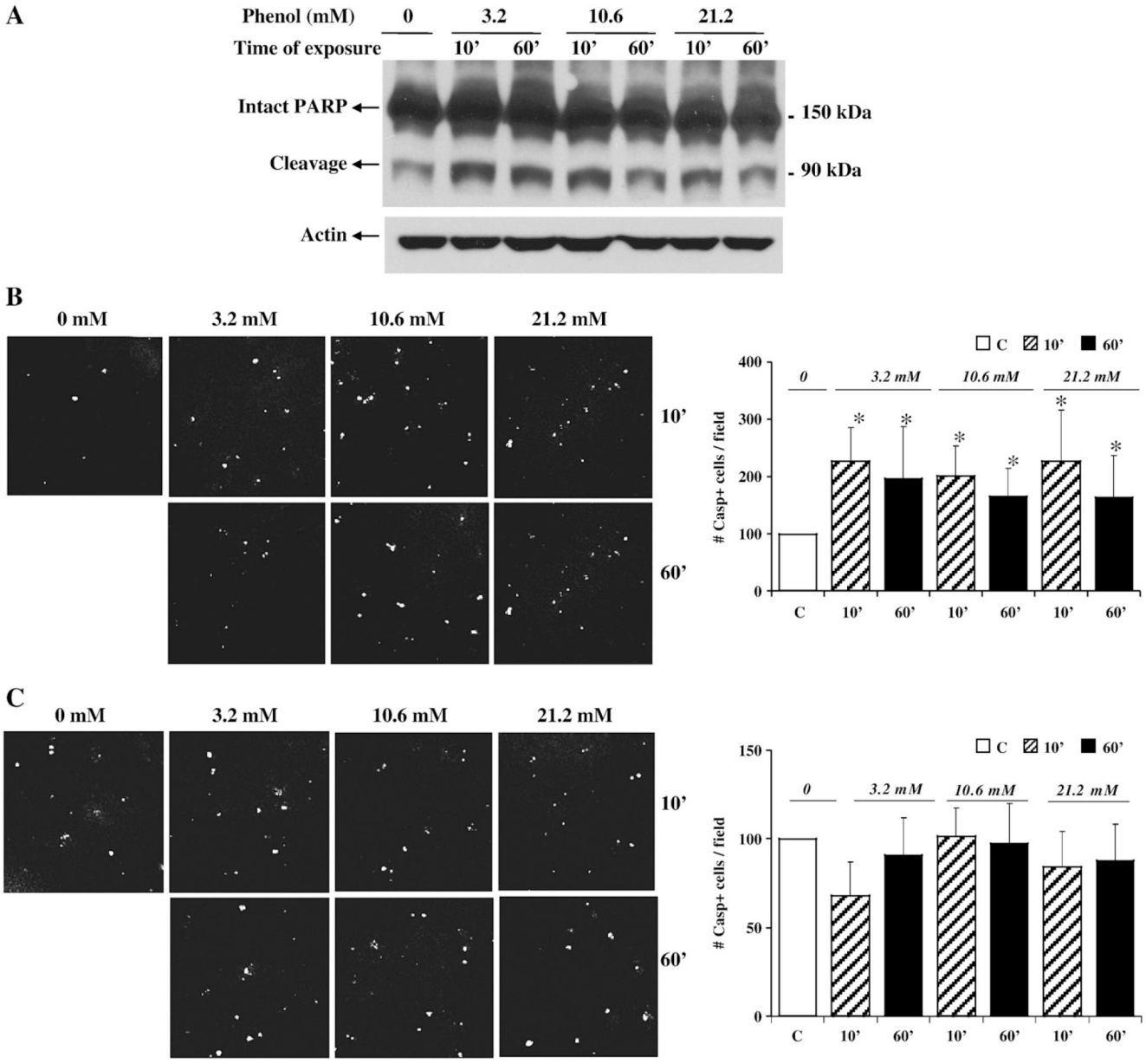

Fig. 6.

Phenol treatment promotes apoptosis. (A) Cellular lysates from SK-CO15 cells treated for 10 and 60 min with different concentration of phenol were analyzed by Western blot to evaluate the expression of apoptosis marker PARP. Intact and cleavage forms of PARP are indicated. Membranes were reblotted for actin as a loading control. (B) TUNEL staining of SK-CO15 cells treated with phenol at 3.2, 10.6, 21.2 mM for 10 and 60 min. The graph represents quantification of data derived from five different fields. The images shown are representative fields of the stained filters. *p<0.05 (post-test following two-way ANOVA) compared with the untreated control. (C) SK-CO15 cells were pretreated with the caspase inhibitor Z-VAD prior to phenol treatment. TUNEL staining was performed. The graph represents quantification of data derived from five different fields. The images shown are representative fields of the stained filters. p = nonsignificant at all concentrations.

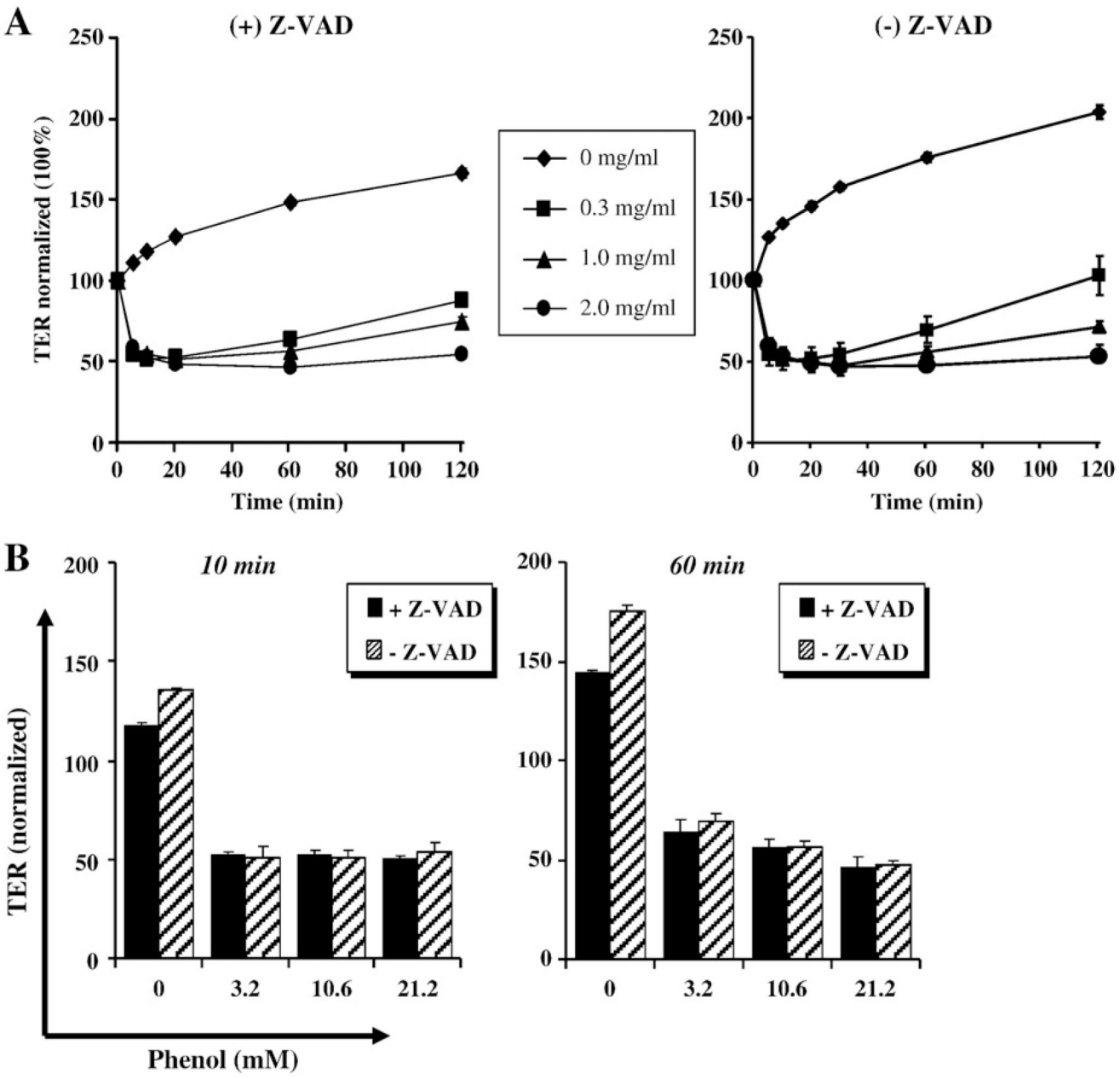

Fig. 7.

Impaired barrier function is independent of apoptosis. SK-CO15 cells pretreated in the presence or absence of ZVAD and treated with phenol as indicated. TER was monitored for a 2-h time course. The quantification of three independent experiments at 10 and 60 min is displayed in the lower graphs.

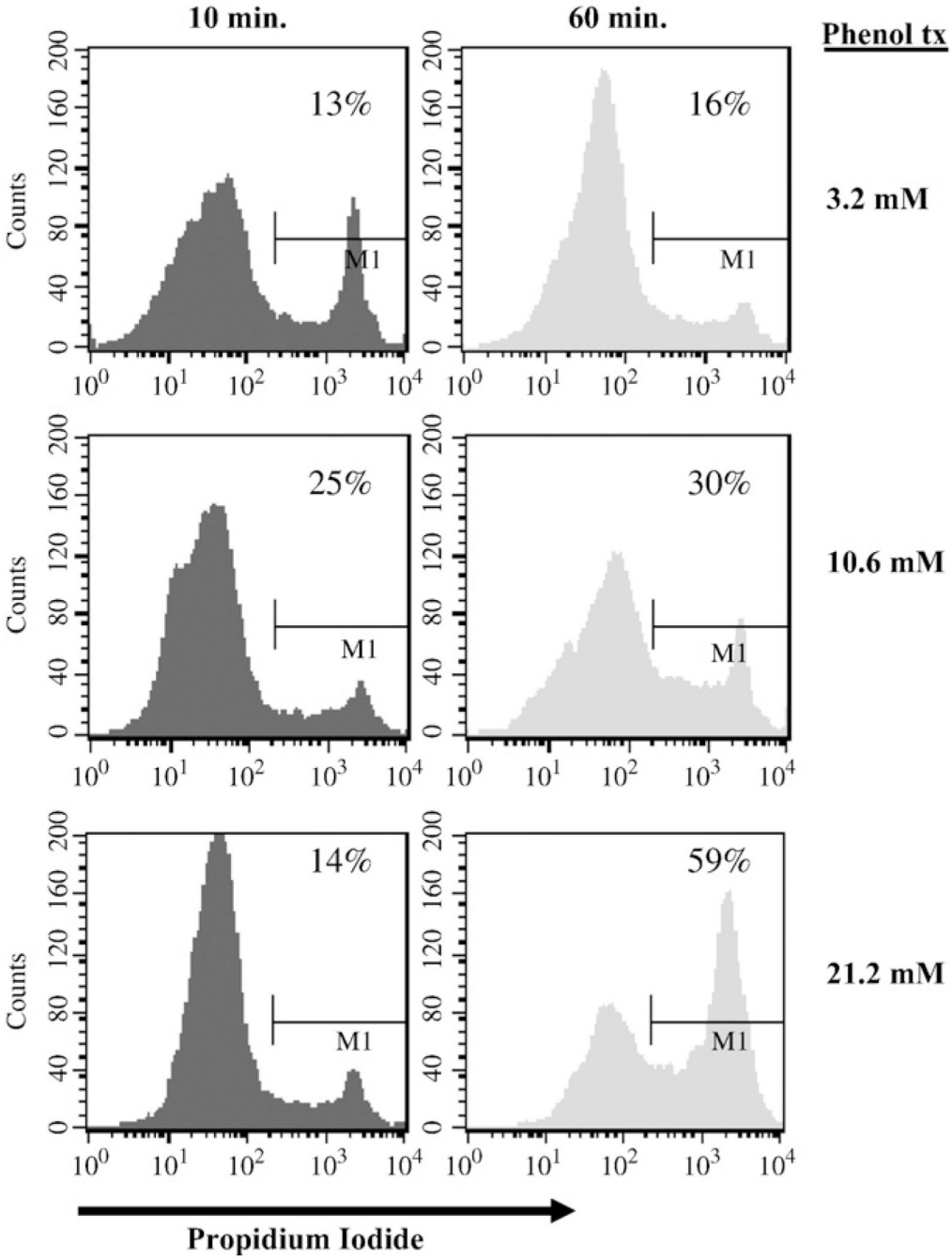

Fig. 8.

Effect of phenol on cellular necrosis. SK-CO15 cells incubated for 10 and 60 min with 3.2, 10.6, 21.2 mM phenol were labeled in suspension with 2 μg/ml PI and processed for flow cytometry using FACSCaliber (BD Biosciences) and Cell Quest software. Data are representative of at least three experiments.

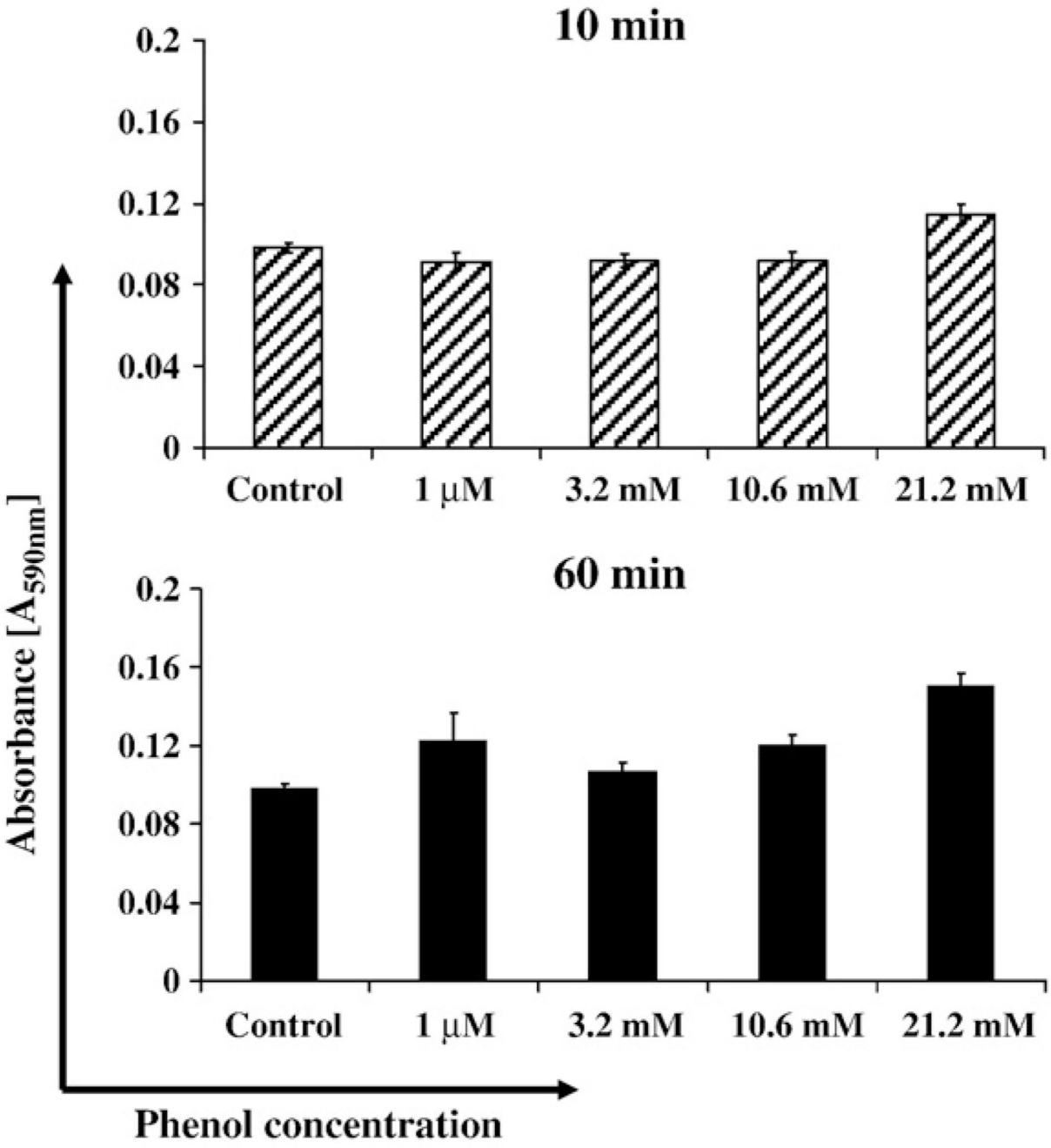

Fig. 9.

Cell viability using MTT assay. SK-CO15 cells incubated in 96-well plates for 10 and 60 min with 1 μM, 3.2 mM, 10.6 mM, 21.2 mM phenol. 10 μl of the MTT labeling reagent was added and incubated for 1 h at 37 °C. Solubilization solution was added (100 μl/well), and data were analyzed by spectrophotometry in a microtiter plate reader at 590 wavelength after an overnight incubation at 37 °C.

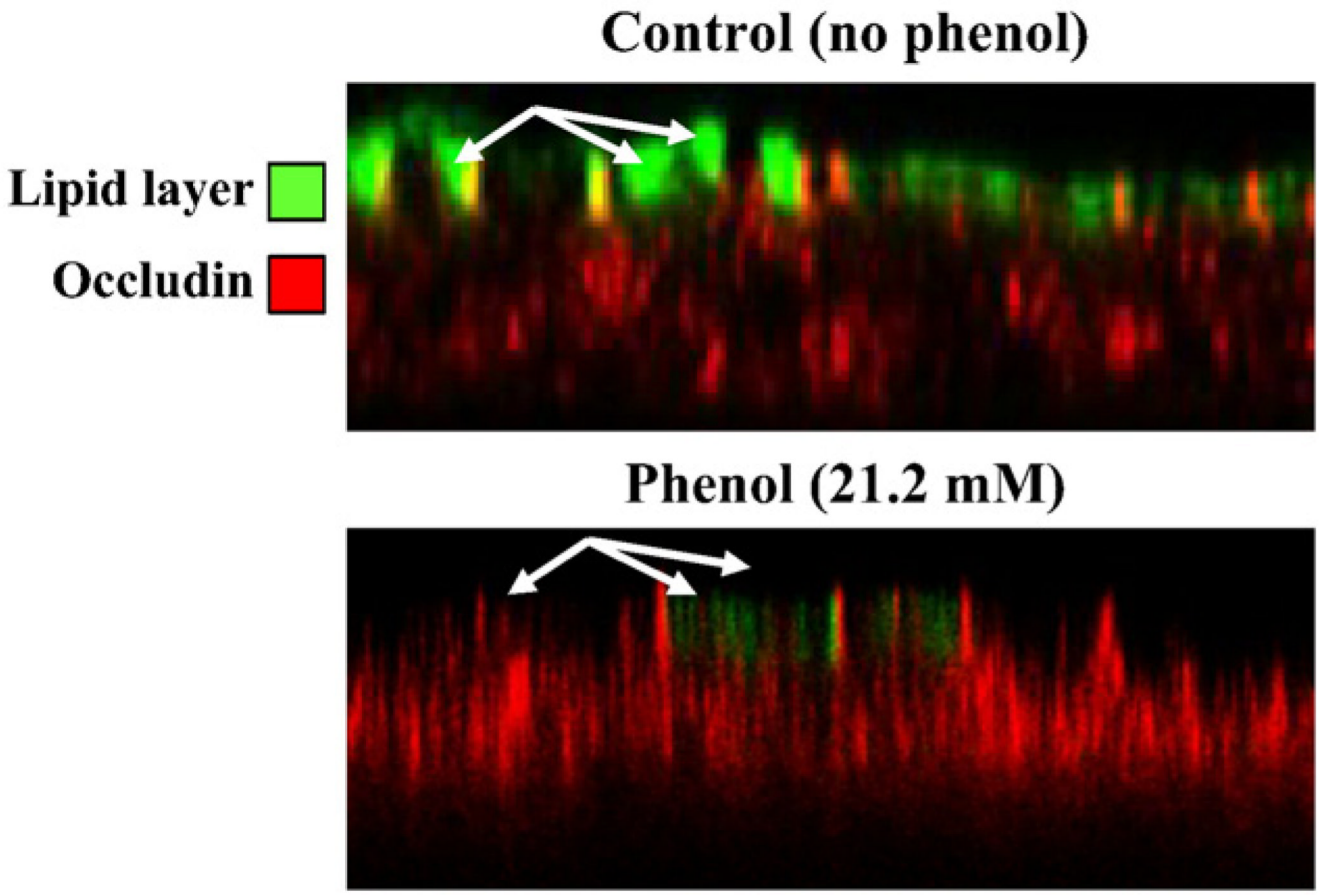

Fig. 10.

Lipid layer integrity using FITC-labeled cholera toxin B. SK-CO15 cells incubated for 10 min with 21.2 mM phenol were labeled in suspension with 2 μg/ml of FITC-labeled cholera toxin B apically to distinguish the lipid layer rich in sphingolipids and cholesterol (green). Cells were fixed/permeabilized with ethanol and stained for the tight junction occludin (red). Note that phenol treatment results in loss of apical FITC-labeled cholera toxin suggesting disruption in membrane polarity/microdomains.